JOURNAL OF MATERIALS SCIENCE 32 (1997) 2071–2075

Electrochemical corrosion behaviours of $Fe_{68}Ni_{14-x}Mo_xSi_2B_{16}$ metallic glasses in 1N HCl and 1N H_2SO_4

B. SESHU, A. K. BHATNAGAR
School of Physics, University of Hyderabad 500046, India
A. VENUGOPAL, V. S. RAJA
Corrosion Science and Engineering, Indian Institute of Technology, Bombay 400076. India

Electrochemical corrosion behaviours of five $Fe_{68}Ni_{14-x}Mo_xSi_2B_{16}$ glasses with $x = 0, 1, 2, 3$ and 4 have been investigated in both 1 N HCl and 1 N H_2SO_4 solutions using potentiodynamic polarization and a.c. impedance spectroscopic techniques. The polarization and impedance results show that all the alloys possess inferior corrosion resistance which has been attributed to the low Ni content on one hand and the absence of passivators such as Cr and P on the other. Interestingly the alloys have been found to show weak passivation in more aggressive HCl and not in relatively mild H_2SO_4 solution. This has been explained in terms of dual behaviours of Mo in HCl and H_2SO_4 based on impedance data and literature work. The present study attempts to correlate impedance data with polarization data through the parameter polarization resistance and indicates that both values are comparable only when an alloy undergoes active dissolution and not when it exhibits passivity.

1. Introduction

Conventional magnetic alloys cannot normally be used for high frequency applications above 100 kHz due to excessive eddy current losses in these frequency ranges. Remarkable soft ferromagnetic properties and high saturation induction combined with high resistivity of Fe-based metallic glasses have opened up new possibilities of their use in high-frequency applications. Extensive studies in this direction have been made on Fe–Ni and Co based alloys with various combinations of several metal and metalloid elements. In this regard the glass $Fe_{40}Ni_{38}Mo_4B_{18}$ [1] have been reported to have better magnetic properties and thermal stability over $Fe_{40}Ni_{40}P_{14}B_6$. Further, it is also found that substantial reduction in Ni with simultaneous addition of Si and a suitable heat treatment can provide excellent properties. Thus $Fe_{75}Ni_4Mo_3B_{16}Si_{12}$ and a series of alloys $Fe_{82-x-y}Ni_xMo_yB_{18-z}Si_z$ [$(0 < x < 12)$, $(0 < y < 6)$, and $(0 < z < 6)$] show that when optimally heat treated provide an a.c. work loss of just 7–8 $W\,kg^{-1}$, exciting power of 13–14 VA/kg, effective permeability of 10^4 at 50 kHz and at an induction of 0.1 T [3]. From the above literature it becomes clear that Fe-based alloys with less Ni and no P are preferred for magnetic applications. However, the application of these glassy alloys for the above purposes is viable only when their thermal and chemical stabilities are guaranteed. A comprehensive programme on the investigation of both these aspects have been undertaken in our laboratory, and this paper concerns the latter aspect. It is well known that P offers excellent corrosion resistance to glasses [4] and Ni being a relatively noble element can also promote corrosion resistance. In the absence of both these elements the corrosion resistance of the glasses can be significantly affected. Hence, it is worthwhile to examine the corrosion behaviour of Fe-based metallic glasses free from P and having low Ni content. In the present investigation, potentiodynamic polarization and a.c. impedance spectroscopy are employed to understand the electrochemical corrosion behaviour of five $Fe_{68}Ni_{14-x}Mo_xSi_2B_{16}$ glasses.

2. Experimental details

Metallic glasses bearing the composition $Fe_{68}Ni_{14-x}Mo_xSi_2B_{16}$ ($x = 0, 1, 2, 3, 4$) in ribbon form of about 5 mm width produced by melt-spinning technique, and as received from Allied signals, USA, were used in the present study. X-ray diffraction patterns of these samples confirmed the amorphous nature. Electrodes for corrosion studies were prepared in the following manner to study selectively either the dull or the bright surface. Strips (10 × 5 mm) were cut from the sample ribbons, cleaned thoroughly with acetone and polished with alumina to remove surface oxides

0022–2461

present, if any. These strips were soldered to a copper wire at one end to provide an electrical contact and subsequently the rough surface was fixed to 20 × 5 mm perspex disc using an epoxy adhesive. The bright side of the samples were thus exposed to the corrosive medium. In addition barring an area (in the range 0.25–0.5 cm^2) the remaining sample was insulated with epoxy resume. Samples were washed in acetone, etched in HCl, rinsed in double distilled water, and immersed in test corrosive media within 5 min of preparation.

The electrochemical cell used for the present study consisted of a 500 ml flat glass beaker with an acrylic lid on the top. Holes are suitably drilled to position a platinum counter electrode, specimen working electrode, and a saturated calomel reference electrode (SCE). During the experiments the cell was maintained at room temperature. 1 N H_2SO_4 and 1 N HCl used as corrosive media were prepared from their respective AR grades and distilled water. The corrosive medium was freely exposed to the atmosphere.

Potentiodynamic polarization measurements were performed using an EG & G PARC potentiostat Model 273 driven by m352 software. The electrode was cathodically polarized at -2 V (SCE) for half a minute, thus facilitating the removal of surface oxides (air-formed films) present, if any. The electrode was allowed to reach a stable corrosion potential, before the potentiodynamic polarization was carried out. A scan rate of 1 mV s^{-1} was applied. All the potentials were measured with respect to SCE.

Impedance data was obtained from a Solatron 1255 frequency response analyser interfaced with EG & G PARC 273 potentiostat and driven by m388 software. Impedance measurements were made in the range 10^5–10^{-2} Hz. Impedance spectra were analysed using Equivcrt commercial software.

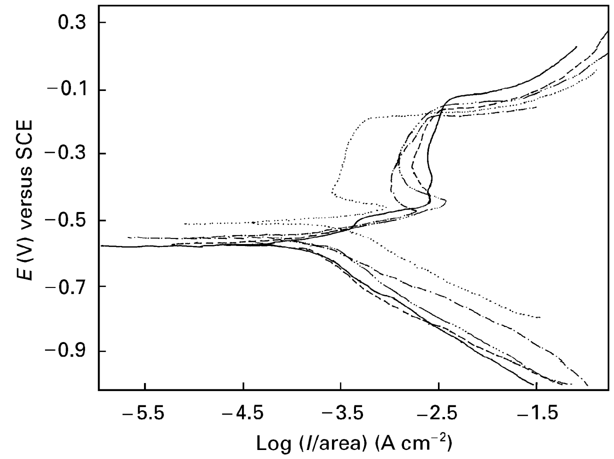

Figure 1 Typical polarization curves of various glasses in 1 N HCl. $x = 0$ (—); $x = 1$ (– ··· –); $x = 2$ (– – –); $x = 3$ (···); $x = 4$ (– · –).

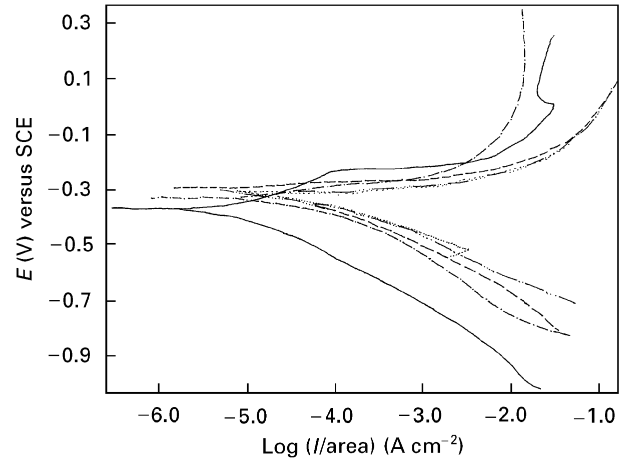

Figure 2 Typical polarization curves of various glasses in 1 N H_2SO_4. See Fig. 1 for key.

3. Results and discussion

Figs 1 and 2 show the polarization behaviours of the metallic glasses under investigation, in 1 N HCl and 1 N H_2SO_4 solutions, respectively. Notably the anodic curves in 1 N HCl show a weak tendency for passivation, although the passive currents exhibited by these alloys are high, lying between 2.5×10^{-4} and 2.7×10^{-3} A cm^{-2}. On the contrary, these alloys show an active dissolution without any revelation of passivity in H_2SO_4. Various kinetic parameters namely, corrosion potential (E_{corr}), corrosion current density (i_{corr}), anodic (β_a) and cathodic (β_c) Tafel slopes derived from these polarization curves are summarized in Tables I and II. Polarization resistances, R_p, calculated from Stern–Geary equation

$$R_P = \frac{\beta_a \beta_c}{i_{\text{corr}}(\beta_a + \beta_c)}$$

using the above parameters are also shown in Tables I and II.

Tables I and II clearly indicate that these alloys exhibit very high corrosion rates in HCl as well as H_2SO_4. Further examination of kinetic parameters

TABLE I Kinetic parameters obtained from the polarization curves for samples $Fe_{18}Ni_{14-x}Mo_xSi_2B_{16}$ in HCl

Sample	E_{corr} (mV)	i_{corr} ($\mu\text{A cm}^{-2}$)	β_a (mV/decade)	β_c (mV/decade)	R_P (ohm cm^2)
$x = 0$	−571	153	109	203	201
$x = 1$	−540	226	71	223	103
$x = 2$	−567	153	79	237	167
$x = 3$	−506	271	31	154	41
$x = 4$	−554	141	70	134	142

TABLE II Kinetic parameters obtained from polarization curves in 1 N H_2SO_4

Sample	E_{corr} (mV)	i_{corr} ($\mu\text{A cm}^{-2}$)	β_a (mV/decade)	β_c (mV/decade)	R_P (ohm cm^2)
$x = 0$	−357	13	125	176	2774
$x = 1$	−290	50	25	103	154
$x = 2$	−310	400	137	137	148
$x = 3$	−317	200	169	169	264
$x = 4$	−331	125	109	109	116

provided in these tables indicate that β_c does not show any systematic variation, although a few Mo containing alloys exhibit lower values than the base alloy with Mo. However, examination of the cathodic curves of Figs 1 and 2 reveal that the cathodic reaction (most likely the H_2 evolution) has a higher reaction rate with Mo addition than without Mo. This is inferred from the fact that most of the cathodic curves are shifted towards the right. Such a tendency is possible only when the exchange current density for the H^+/H equilibrium ($i_{OH^+/H}$) increases with Mo addition. In contrast to β_c there is a significant reduction in β_a due to Mo addition both in HCl and H_2SO_4. These observations emphasize the fact that mere amorphous nature of the alloy is inadequate to provide resistance towards corrosion. Presence of one or more passivating elements like Cr and P in the alloys is a necessary condition to extend the benefit of amorphous structure of alloys. Thus Fe–Cr–Mo–B in 6 N HCl [5], Fe–xMo–13P–7C in 1 N HCl [6] and Fe–xMo–18C [7] in 1 N HCl have been reported to exhibit excellent corrosion resistance. The present alloys fail to exhibit corrosion resistance on two accounts. Firstly, the metalloid B and Si are inferior to P [4] in offering corrosion resistance. Secondly, unlike $Fe_{40}Ni_{38}Mo_4B_{18}$ and $Fe_{39}Ni_{39}Mo_4Si_6B_{12}$ [8] glasses that possess good resistance to corrosion, the present alloys do not possess high Ni which is, relatively, a nobler element than Fe. From the tables there appears to be no systematic change in i_{corr} in HCl medium with the variation in x. A possible improvement in corrosion resistance due to the rise in Mo is offset by the simultaneous reduction in Ni content of the alloy. With respect to H_2SO_4 solution a gradual decrease in corrosion resistance occurs as x is increased from 0 to 2. On further increasing x a steady rise in corrosion resistance is noticed. This indicates that at higher x values Mo has a higher beneficial effect than Ni. Indeed, in a systematic study of Fe–Mo crystalline alloys Ambrose [9] has shown that if the Mo content of Fe–Mo alloy exceeds 5 wt % it offers good corrosion resistance, while at lower values Mo tends to be detrimental, agreeing with the present trend. Nevertheless, the effective role of Mo is decided by the complementary role played by other alloying elements. This becomes clear from the fact that in austenitic stainless steels even 2 wt % Mo brings out a significant improvement in corrosion resistance and passivity, as has been shown by AISI 304 and 316 ss while even 5 wt % Mo brings out only a marginal change in Fe–Mo alloys [9].

Electrochemical investigation of the present glassy alloy further enables an understanding of the role Mo plays in ferrous alloys towards passivity when Cr is not present. This has become possible now since the homogeneous single phase nature is retained in spite of high Mo content, which would be difficult if crystalline Fe-based alloys are chosen. This is because in crystalline Fe-based alloys the solubility of Mo is low. As a consequence additional phases would be formed, which by itself would be a factor influencing corrosion behaviour over the intended compositional variation brought about by Mo.

The passivation behaviour of these glasses were further examined using a.c. impedance spectroscopy. Nyquist plots obtained at E_{corr} in 1 N HCl and 1 N H_2SO_4 solutions respectively are presented in Figs 3 and 4. As these alloys exhibit an apparent tendency to passivate in HCl their impedance behaviours were also studied at -456 and -200 mV (SCE) which lie in the passive region. The corresponding Nyquist plots, respectively, are shown in Figs 5 and 6. In HCl, barring a few cases, existence of two overlapping capacitive loops are discernible in Nyquist plots obtained at E_{corr}, -456 and -200 mV (SCE). Nyquist plots for the glassy alloys obtained in H_2SO_4 differ from that obtained in HCl by displaying a capacitive loop followed by an inductive loop. The resistance values corresponding to first and second semicircles, namely R1 and R2, are summarized in Tables III and IV for HCl and H_2SO_4 media, respectively. R1 has

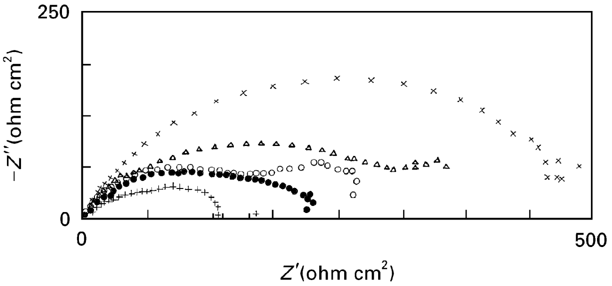

Figure 3 Nyquist representation of impedance data at E_{corr} in 1 N HCl. $x = 0$ (+); $x = 1$ (△); $x = 2$ (●); $x = 3$ (×); $x = 4$ (○).

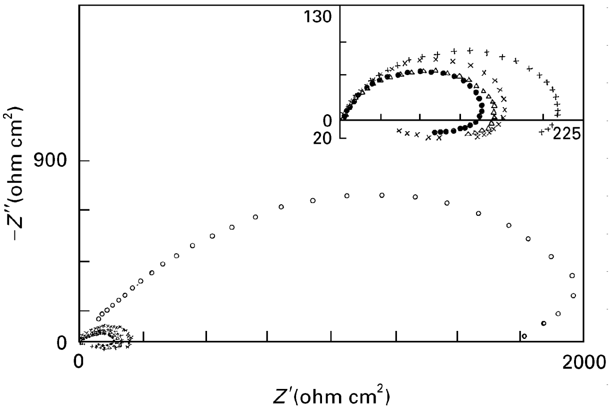

Figure 4 Nyquist representation of impedance data at E_{corr} in 1 N H_2SO_4. $x = 0$ (○); $x = 1$ (×); $x = 2$ (△); $x = 3$ (+); $x = 4$ (●).

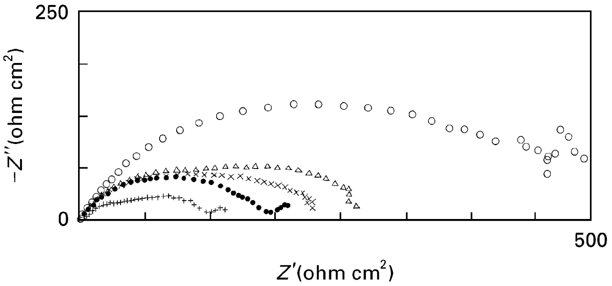

Figure 5 Nyquist representation of impedance data at -456 mV (SCE) in 1 N HCl. $x = 0$ (+); $x = 1$ (○); $x = 2$ (×); $x = 3$ (●); $x = 4$ (△).

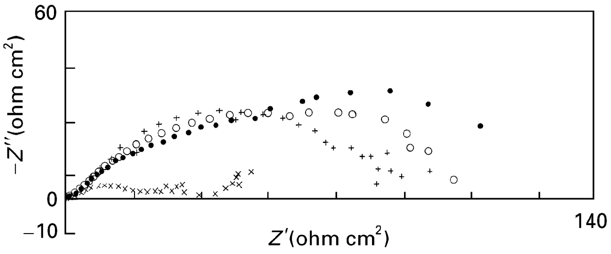

Figure 6 Nyquist representation of impedance data at −200 mV (SCE) in 1 N HCl. $x = 0$ (+); $x = 1$ (○); $x = 2$ (×); $x = 3$ (●).

TABLE III Variations in R1 and R2 values obtained from the impedance curves in 1 N HCl medium

Sample	R1 (ohm cm^2)	R2 (ohm cm^2)	R_P = R1 + R2 (ohm cm^2)
$x = 0$	101	41	141
$x = 1$	325	95	420
$x = 2$	195	33	228
$x = 3$	485	–	485
$x = 4$	184	105	289

TABLE IV Variations in R1 and R2 values obtained from the impedance curves in 1 N H_2SO_4 medium

Sample	R1 (ohm cm^2)	R2 (ohm cm^2)
$x = 0$	2060	–
$x = 1$	145	–
$x = 2$	148	49
$x = 3$	212	59
$x = 4$	92	48

TABLE V Variations in R1 and R2 values obtained from the impedance curves at a fixed potential of −456 mV in 1 N HCl medium

Sample	R1 (ohm cm^2)	R2 (ohm cm^2)	R_P = R1 + R2 (ohm cm^2)
$x = 0$	77	40	117
$x = 1$	452	–	452
$x = 2$	190	37	227
$x = 3$	170	–	170
$x = 4$	185	83	268

TABLE VI Variations in R1 and R2 values obtained from the impedance curves at a fixed potential of −200 mV in 1 N HCl medium

Sample	R1 (ohm cm^2)	R2 (ohm cm^2)	R_P = R1 + R2 (ohm cm^2)
$x = 0$	73	17	90
$x = 1$	76	20	96
$x = 2$	85	20	105
$x = 3$	18	62	80
$x = 4$	83	24	107

TABLE VII Comparison of polarization resistance (R_P in ohm cm^2) values obtained from polarization experiments and impedance experiments at E_{corr} in 1 N HCl and 1 N H_2SO_4 solutions

Samples	Polarization curves in 1 N HCl	Impedance curves in 1 N HCl	Polarization curves in 1 N H_2SO_4 (R1)	Impedance curves in 1 N H_2SO_4
$x = 0$	201	142	2774	2060
$x = 1$	103	420	154	145
$x = 2$	167	228	148	148
$x = 3$	41	485	264	212
$x = 4$	142	289	116	92

been taken as R_p since R2 corresponds to inductive semicircle. Similarly the resistance values calculated at potentials −456 and −200 mV are summarized in Tables V and VI.

The appearance of high and low frequency capacitive loops has been attributed respectively due to dielectric relaxation of films and faradaic processes occurring on the electrode surface [10]. With regards to inductive loops no definite processes can be assigned. Literature, however, indicates that inductive loop in Nyquist representation occurs as a result of either of the following reasons namely pitting [11], relaxation of reaction intermediates [12] and increase in anionic defects over cationic defects [13].

The fact that the glassy alloys exhibit a high frequency capacitive loop in addition to a low frequency capacitive loop suggests that some sort of film exists on these alloys in HCl, further supporting polarization studies. Therefore, it seems that Cl^- ions promote formation of corrosion/passive film while SO_4^{2-} ions do not favour such film formation. In this context it is worthwhile to mention the fact that Ogawa *et al.* [14] had detected the presence of Mo in the film formed on several Mo containing stainless steels passivated in H_2SO_4 medium only if Cl^- are added to the solution. This suggests that Cl^- differs from SO_4^{2-} with respect to film formation. Further more Ambrose [9] also proposed that Mo minimizes localized corrosion by the formation of salt film on Fe–Mo alloys. This happens when the MoO_4^{2-} concentration in the vicinity of the electrode surface is high. The possibility of salt film formation seems to gain credence from the fact that the metallic glasses in HCl do not show any systematic variation in R_P value with variation in x value. Even for a single composition, the values differ from one specimen to another to some extent. This is because the nature and adherence of salt film formed on the alloy surface will depend more on local chemistry and surface nature than on alloy chemistry. It is also to be noted that the resistance offered by these films at the passive potential (−200 mV) is much lower than that obtained at E_{corr}. Mo seems to operate through a different mechanism to enhance passivity in H_2SO_4. The electron spectroscopy for chemical analysis (ESCA) work of Ogwa *et al.* [14] shows that Mo enriches an alloy surface with high Ni or Cr when passivated in H_2SO_4. The high Ni and/or Cr on the surface in turn lower passive current and Mo *per se* does not contribute to passivity. Viewed in this perspective the present glasses fail to show passivity because they do not have either high Ni content as in

$Fe_{39}Ni_{39}Mo_4Si_6B_{12}$ [8] Cr [5] or P [6]. On the other hand absence of these elements results in a gradual increase in corrosion rate. This is clear from i_{corr} values listed in Table II and R_P values listed in Table IV.

In the present study an attempt has been made to find out to what extent polarization data correlate with that of impedance data using R_P as a parameter. Table VII compares the R_P values obtained through Stern–Geary relationship with that obtained from impedance spectroscopy in 1 N HCl and 1 N H_2SO_4, respectively, at E_{corr}. It is obvious from the data that under active dissolution of alloys (in H_2SO_4) there is a good correlation between the two data and on the contrary the two values do not correlate with one another if the alloys become passive. Thus it brings out a fact that R_P can not be considered to be a factor indicating corrosion resistance of the alloy if the alloy passivates and more so if it forms salt film.

4. Conclusions

1. The present glassy alloys exhibit poor corrosion resistance both in 1 N HCl and 1 N H_2SO_4 solutions.
2. With increase in Mo content the passivity of the alloy increases in HCl, though the passive current is quite high, while no such passivity is seen in H_2SO_4
3. The mechanism of alloys dissolution in presence of Mo in HCl seems to be different from that of H_2SO_4
4. A good correlation seems to exist between the polarization resistance values obtained by impedance and polarization techniques when the alloys undergo active dissolution and not when they possess passivity.

5. Acknowledgements

One of the authors, BS is grateful to the Council of Scientific and Industrial Research, CSIR, India for providing the Senior Research Fellowship (SRF). BS and AKB are grateful to the Department of Atomic Energy (DAE) India, for supporting this work.

References

1. T. EGAMI, P. J. FLANDENS and C. D. GRAHAM Jr, in American Institute of Physics (AIP) Conference Proceedings No. 24, edited by C. D. Graham Jr, G. M. Lander and J. J. Rhyne (New York, 1975) p. 697.
2. R. HASEGAWA and C. P. CHEN, US patent no. 4152144 (1979).
3. R. HASEGAWA, G. E. FISH and V. R. V. RAMANAN, in Proceedings of the 4th International Conference on Rapidly Quenched Metals edited by T. Masumoto and K. Suzuki (Japan Institute of Metals, Aoba Aramaki, Sendai, Japan, 1981) Vol. 2, p. 929.
4. M. NAKA, K. HASHIMOTO and T. MASHUMOTO, *J. Non-Cryst. Solids* **28** (1978) 403.
5. K. ASAMI, M. NAKA, K. HASHIMOTO and T. MASUMOTO, *J. Electrochem. Soc.* **127** (1980) 2130.
6. M. NAKA, K. HASHIMOTO and T. MASUMOTO, *J. Non-Cryst. Solids* **29** (1978) 61.
7. M. NAKA, K. HASHIMOTO, A. INONE and T. MASUMOTO, *J. Non-Cryst. Solids* **31** (1979) 347.
8. V. S. RAJA, KISHORE and S. RANGANATHAN, *Corrosion* **44** (1988) 263.
9. J. R. AMBROSE, *Corrosion* **34** (1978) 27.
10. M. SEO and N. SATO, Corrosion paper No. 138, NACE, New Orleans, LA, 1989.
11. J. BESSONE, C. MAYER, K. JUTTNER and W. J. LORENZ, *Electrochim. Acta* **28** (1983) 171.
12. F. MANSFELD and J. C. S. FERNANDES, *Corrosion Sci.*, **34** (1993) 2105.
13. I. EPELBOIN, M. KEDDAM and J. C. LESTRADE, *Trans. Farad. Soc.* **56** (1981) 264.
14. R. D. AMSTRONG and K. EDMONDSON, *Electrochim. Acta* **18** (1973) 937.

Received 19 January
and accepted 31 July 1996